This paper is included in the MRS International Materials Research Conference, 9-12 June 2008, Chongqing, China.

MODELLING HIGH TEMPERATURE FLOW STRESS CURVES OF TITANIUM ALLOYS

Z. Guo, N. Saunders, J.P. Schillé, A.P. Miodownik
Sente Software Ltd, Surrey Technology Centre, Guildford, GU2 7YG, U.K.

Keywords: Titanium alloys, Strength, Flow stress curve, Material data, Processing simulation.

Abstract

This paper describes the development of a computer model for the calculation of high temperature flow stress curves of titanium alloys. Two competing mechanisms for deformation, either dominated by dislocation glide or dominated by dislocation climb, were considered in the calculation. Validation has been carried out for a variety of titanium alloys over a wide range of temperatures and strain rates. The flow stress data can be used as replacement to the constitutive equations in computer-aided-engineering simulation.

Introduction

Thermo-mechanical processing simulation requires critical material data such as strength and stress-strain curves (or flow stress curves). The traditional way of obtaining such data is through experimentation, which is expensive and time-consuming, because mechanical properties are temperature and strain rate dependent. It is therefore of no surprise that lack of material data has been a common problem for computer-aided-engineering (CAE) simulation tools.

CAE simulation packages normally provide a range of constitutive equations that describe stress as a function of temperature, strain and strain rate, e.g. the widely used Johnson-Cook model [1]. However, the choice of the equations used can significantly affect the simulation results [2,3,4], as each has its own limitations and can only work in a certain range [5]. Not only do users have to decide which equation to use, but they also have to determine the values of the material parameters used in the equation, where experimental flow stress data is a pre-requisite [4,6,7].

The present paper looks at material flow from the viewpoint of the actual mechanisms during deformation. Two competing mechanisms for deformation, i.e. either dominated by dislocation glide (DDG) or dominated by dislocation climb (DDC), were considered in the investigation. After a recapitulation of previous work on the calculation of high temperature strength, the paper focuses on calculating stress-strain curves in different temperature and strain rate regimes. The advantages of using such an analytical approach to replace subjectively selected constitutive equations are discussed.

High Temperature Strength

Generally speaking, the strength of an alloy decays monotonically with increasing temperature until a critical temperature is reached, above which there is a sharp fall in strength. This sharp drop in strength is invariably due to a change of deformation mechanism from being dominated by dislocation glide (DDG) at low temperatures to being dominated by dislocation climb (DDC) at higher temperatures [8,9]. The latter is usually the controlling mechanism for creep. Different strength models have been employed in previous work [8,9] to account for the two different mechanisms. Whichever has the lower resistance to deformation controls the final strength of

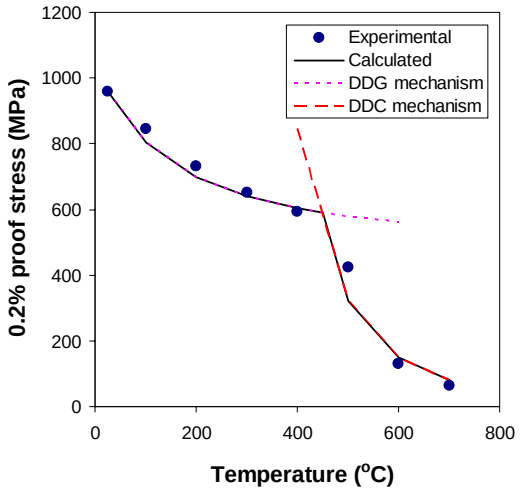

Fig. 1. Comparison between experimental and calculated proof stress for titanium alloy IMI 318 (Ti-6Al-4V).

the alloy. The two regions are clearly shown in Fig. 1, using the 0.2% proof stress vs. temperature ($\sigma_{0.2}$-T) plot of an IMI 318 alloy (equivalent to Ti-6Al-4V) as an example. The strain rate used in calculation is taken as 3.33×10^{-5} s^{-1} (i.e. 0.002/min). This is the typical value for tensile testing and hereafter will be denoted as $\dot{\varepsilon}_0$. The strain corresponding to $\sigma_{0.2}$ is 0.002, hereafter denoted as ε_0. The calculation of strength at elevated temperatures forms the basis of the following calculation of stress-strain curves.

Stress-Strain Curve

Stress as a result of deformation is dependent on strain rate ($\dot{\varepsilon}$), strain (ε), and temperature (T), which can be described by the following function:

$$\sigma = f(\dot{\varepsilon}, \varepsilon, T) \tag{1}$$

The $\sigma_{0.2}$-T plot shown in Fig. 1 is a special case of Eq. 1 where $\dot{\varepsilon}$ and ε are fixed as ε_0 and $\dot{\varepsilon}_0$, respectively. The stress-strain (σ-ε) curve is another special case of Eq. 1 where T and $\dot{\varepsilon}$ are fixed. With the recognition of the switch of mechanism in the $\sigma_{0.2}$-T plot, one would expect to see such a switch in a σ-ε curve as well. This is schematically shown in Fig. 2, where deformation starts in the DDG-controlled region, and then above a critical strain (ε_t) the creep-controlled flow takes over. In reality, apart from the mixed mode shown in Fig. 2, the observed σ-ε curve can be dominated by either of the two mechanisms. The procedures for the calculation of σ-ε curves in the two regions are described below, respectively.

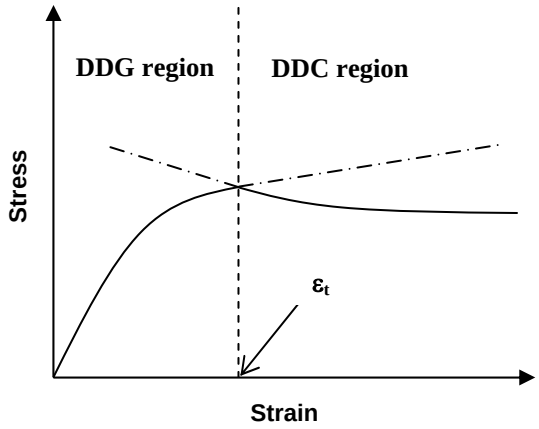

Fig. 2. Change of deformation mechanism from DDG to DDC in a high temperature stress-strain curve at the critical transition strain (ε_t)

Stress-strain curve in DDG region

Stress-strain curve can be considered as the sum of an elastic region and a plastic region. In the elastic region, the stress is proportional to the strain according to Hooke's law. The plastic region is where strain hardening occurs. Stress is related to strain via work hardening coefficient n and constant K:

$$\sigma = K\varepsilon^n \tag{2}$$

The value of n can be estimated from σ_p via the following relationship:

$$n = a\exp(b\sigma_{0.2}) \tag{3}$$

where a and b are material constants dependent of alloy type. Their values have been fitted empirically for a wide range of titanium alloys [10]. When $\sigma_{0.2}$ is known, n is known. As $\sigma_{0.2}$ is the stress at strain ε_0, K can then be calculated as:

$$K = \sigma_{0.2} / \varepsilon_0^{\,n} \tag{4}$$

Most materials are sensitive to the rate of deformation, the so-called strain rate hardening. This behaviour often obeys a power law via strain rate sensitivity m. Strain rate hardening can be combined with strain hardening and described as below:

$$\sigma = K\varepsilon^n\dot{\varepsilon}^m \tag{5}$$

When $\sigma_{0.2}$ corresponds to $\dot{\varepsilon}_0$, the 0.2% proof stress at strain rate $\dot{\varepsilon}$ can be calculated as:

$$\sigma = \sigma_p(\dot{\varepsilon} / \dot{\varepsilon}_0)^m \tag{6}$$

Therefore the stress at any given strain and strain rate can be calculated, which gives the σ-ε curve at any strain rate and temperature. Fig. 3 is the calculated stress-strain curves for an Ti6242 alloy at room temperature (RT) and 482°C. The strain rate used is $3.33\text{x}10^{-5}$ s^{-1}. As this is in the DDG-controlled region, only strain hardening is observed.

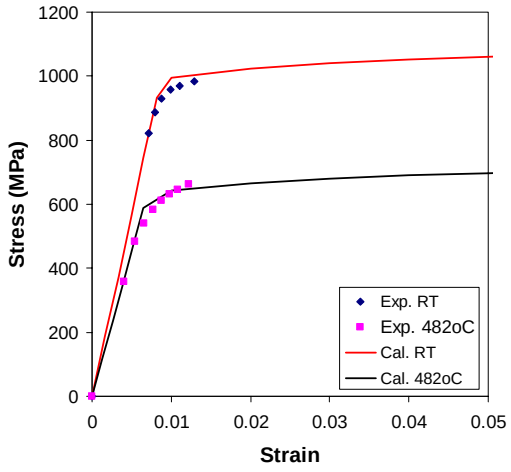

Fig. 3. Comparison between experimental and calculated stress-strain curves for an Ti6242 alloy at RT and 482°C. The strain rate used is $3.33\text{x}10^{-5}$ s^{-1}.

Flow stress curve in DDC region

When in the DDC region where deformation is creep-controlled, creep curves are usually used to describe strain as a function of stress, temperature and time t, i.e.:

$$\varepsilon = g(T, \sigma, t) \tag{7}$$

Since there are only two independent variables in strain, strain rate and time, Eq. 7 and Eq. 1 are essentially equivalent. A creep curve is therefore just another special case of Eq. 1 where T and σ are fixed.

A typical creep curve contains three stages: primary, secondary and tertiary. The creep model to describe the primary creep follows the work of Li [11]:

$$\dot{\varepsilon}_p = \frac{\dot{\varepsilon}_s}{K_0} \ln\left[1 + \frac{\dot{\varepsilon}_i - \dot{\varepsilon}_s}{\dot{\varepsilon}_s}(1 - e^{-K_0 t})\right] \tag{8}$$

where $\dot{\varepsilon}_p$ and $\dot{\varepsilon}_s$ are respectively the primary and secondary creep rates, $\dot{\varepsilon}_i$ is the initial creep rate and K_0 is an empirically evaluated materials constant. $\dot{\varepsilon}_i$ is set to be proportional to $\dot{\varepsilon}_s$ in the present study [12]. To account for the tertiary stage an empirical model is used, which relates the tertiary creep rate to the secondary rate and the creep rupture life:

$$\dot{\varepsilon}_t = \left[2C_d t(t/R_l)^4\right]\dot{\varepsilon}_s \tag{9}$$

where $\dot{\varepsilon}_t$ is the tertiary creep rate, C_d is a "damage constant" and R_l is the rupture life, which can be readily calculated from $\dot{\varepsilon}_s$ via a Monkman-Grant type relationship [9].

Solution to Eqs. 8 and 9 relies on prior knowledge of the secondary creep rate, which can be calculated via the equation below [9,13,14]:

$$\dot{\varepsilon}_s = AD(Gb/RT)(\sigma/E)^{n'} \tag{10}$$

where A is a material constant, D the diffusion coefficient, b the Burgers vector, σ now termed as the applied stress, G and E the shear and Young's modulus of the matrix at the creep temperature, respectively. The stress exponent n' is related to the mechanism of the creep and was set as 4 for both alpha and beta phases in titanium alloys. Almost all of the parameters in Eq. 10 can be calculated [9,15]. This leaves A as the only adjustable parameter, fitted with experimental results.

With the creep rates for all the three stages known from Eqs. 8, 9 and 10 for a given stress and temperature, strain ε as a function of time t, i.e. the creep curve, can be calculated as below:

$$\varepsilon = (\dot{\varepsilon}_p + \dot{\varepsilon}_s + \dot{\varepsilon}_t)t \tag{11}$$

At a fixed temperature, the stress-strain curves $\sigma = f(\varepsilon, \dot{\varepsilon})$ and the creep curves $\varepsilon = f(\sigma, t)$ are effectively forming the same surface in the 3D space of axes σ, ε, and $\dot{\varepsilon}$ or t. If a series of creep curves corresponding to different stresses are known, the stress-strain curve at a fixed strain rate can be obtained. The calculated flow stress curves of grade Ti-6Al-4V (ELI) are shown in Fig. 4

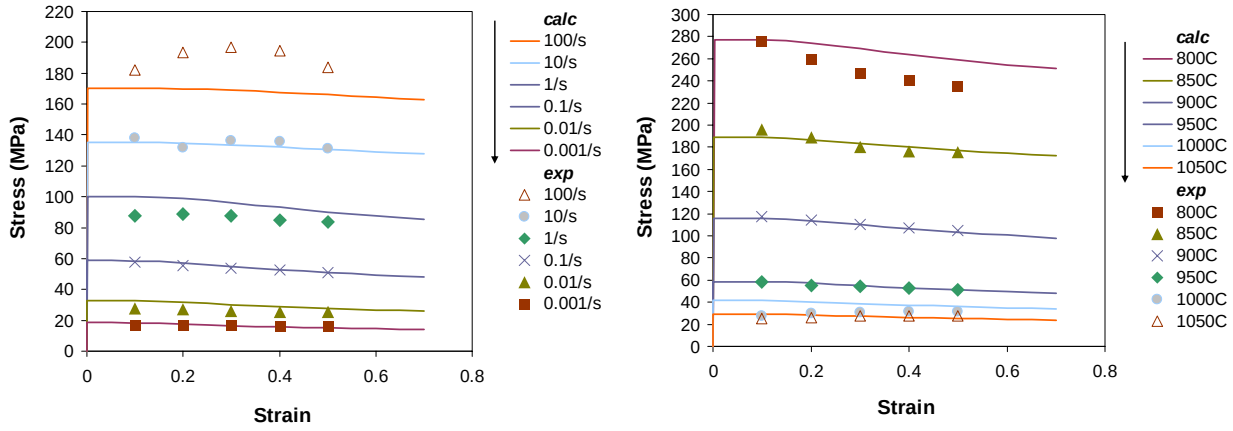

Fig. 4 . Comparison between experimental and calculated flow stress curves for a Ti-6Al-4V (ELI) alloy at (a) 950ºC with various strain rates, and (b) various temperatures with strain rate 0.1/s.

together with experimental data, corresponding to various strain rates at 950°C and various temperatures at strain rate 0.1 s^{-1}, respectively. In all cases there is no detectable DDG region.

Applications of Model

A computer model has been developed to combine the calculation of stress-strain curves in the two regions as described in the previous session. One can now calculate the stress-strain curve at any given temperature and strain rate. The switch of deformation mode shown in Fig. 2 is not observed in Figs. 3 and 4. This is because the value of ε_t can be quite different depending on temperature and strain rate. Generally speaking, higher temperatures and lower strain rates results in smaller ε_t. Such change in the shape of stress-strain curve is clear shown in Fig. 5, using an Ti-6Al-4V alloy as an example. The strain rate used in the calculation of Fig. 5(a) is 3.33×10^{-5} s^{-1}, and the temperature for Fig. 5(b) is 700°C. Switch of deformation mode is clearly observed at 570°C in Fig. 5(a) and 0.1 s^{-1} in Fig. 5(b), respectively. It should be noted that flow softening is often suggested to be due to recrystallisation. However, as clearly shown here, flow softening is a natural result of the DDC-controlled deformation whether or not recrystallisation takes place.

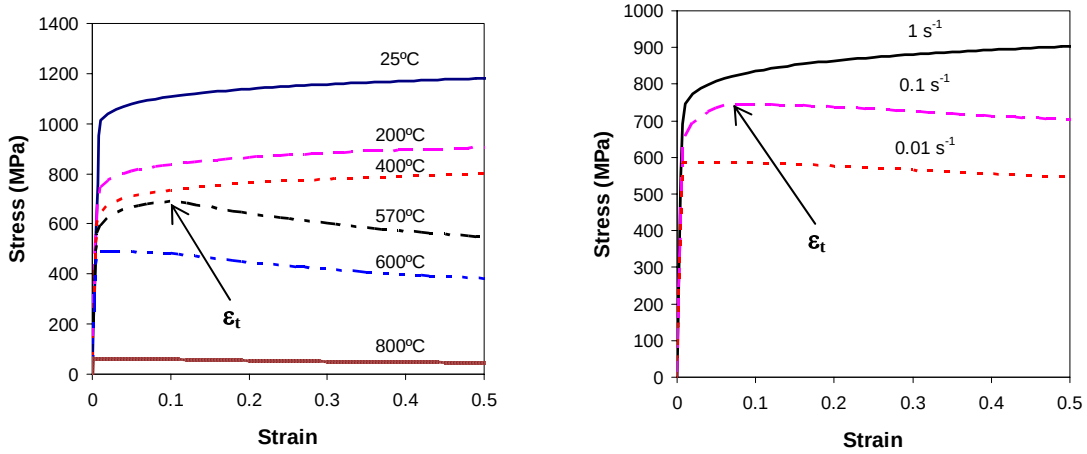

Fig. 5. Calculated flow stress curves for a Ti-6Al-4V alloy at (a) various temperatures with strain rate 3.33×10^{-5} s^{-1}, and (b) 700ºC with various strain rates. Switch of deformation mechanism is clearly marked when taking place at 570°C in (a) and 0.1 s^{-1} in (b), respectively.

The consideration of such a switch in deformation mode allows strain hardening and flow softening to be naturally accounted for in the calculation of stress-strain curves. The problems associated with picking the right constitutive equation and assigning correct values to the material parameters involved have therefore been effectively removed. The predictive capability of the model in flow stress calculation for a wide range of Ti-alloys is demonstrated in Fig. 6, which have been tested over a wide range of temperatures and strain rates. The model has been implemented in computer software JMatPro [15]. Links with many CAE simulation packages have been established and the calculated flow stress data can now be organized in such a format that can be directly read by such packages [16].

Summary

The paper reports the development of a computer model that is able to calculate the high temperature strength and stress-strain curves in titanium alloys. Two mechanisms of deformation

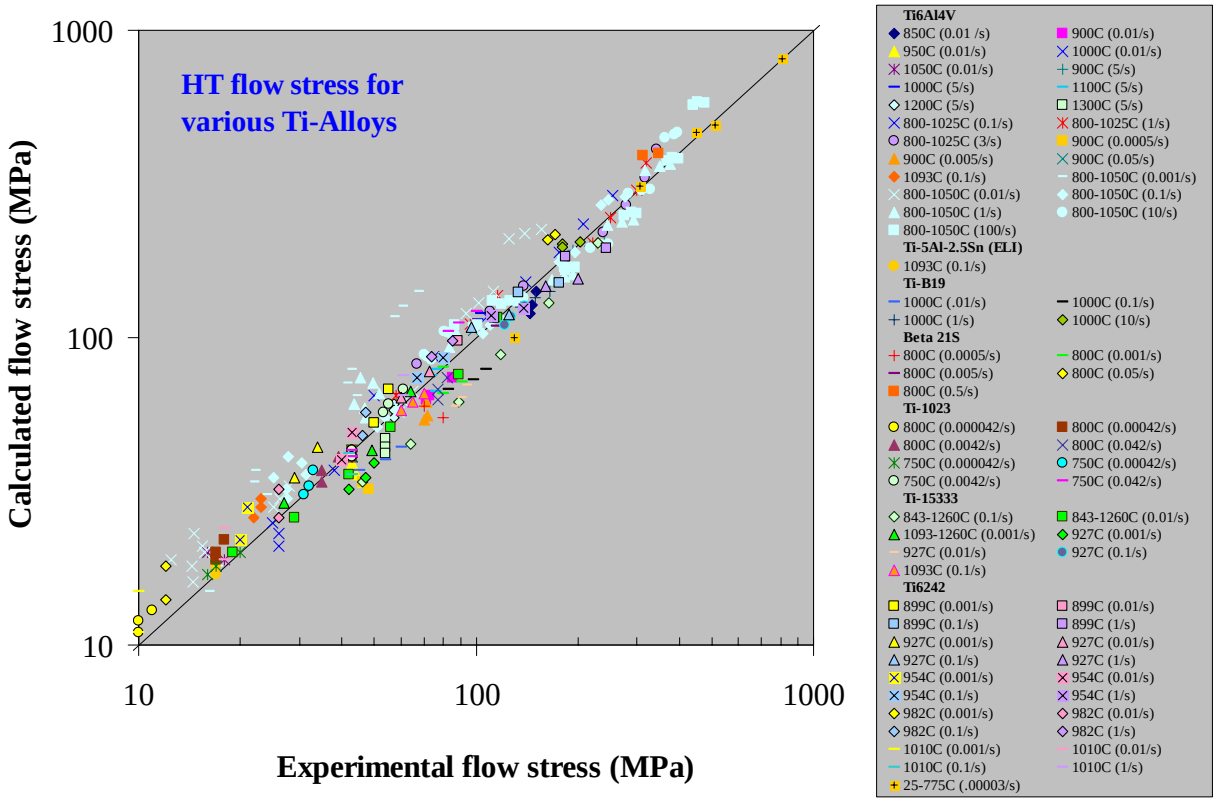

Fig. 6. Comparison between experimental and calculated flow stress for various titanium alloys at various temperatures and strain rates.

were considered in the model, dominated by either dislocation glide or dislocation climb. The model can therefore generate stress-strain curves very different in shape, with strain hardening, flow softening or a mixture of the two. The problem caused by lack of material data in CAE processing modelling has been largely overcome.

References

[1] G.R. Johnson, W.H. Cook, in: Proceedings of the Seventh International Symposium on Ballistic, The Hague, The Netherlands, 1983, pp.541-547.

[2] D. Umbrello, R. M'Saoubi, J.C. Outeiro, International Journal of Machine Tools and Manufacture 47 (2007) 462–470

[3] D. Umbrello, J. Mater. Process. Tech. (2007), doi:10.1016/j.jmatprotec.2007.05.007

[4] A. Söderberg, U. Sellgren, in: NAFEMS World Congress 2005, Malta, 17-20 May 2005.

[5] R. Liang, A.S. Khan, International Journal of Plasticity 15 (1999) 963-980.

[6] Y.B. Guo, J. Mater. Process. Tech. 142 (2003) 72-81.

[7] B. Langrand, P. Geoffroy, J.L. Petitniot, J. Fabis, E. Markiewicz, P. Drazetic, Aerospace Science and Technology, 1999, no. 4,215-227.

[8] Z. Guo, N. Saunders, A.P. Miodownik, J.P. Schillé, Materials Science Forum, 546-549 (2007) 1319-1326.

[9] Z. Guo, N. Saunders, A.P. Miodownik, J.P. Schillé, Rare Metal Materials and Engineering, 35 (Sup. 1) (2006) 108-111.

[10] Unpublished research, Sente Software Ltd., 2003.
[11] J.C.M. Li, Acta Metall. 11 (1963) 1269.
[12] F. Garofalo, W.F. Domis and F. Von Gemmingen, Trans. Met. Soc. AIME 230 (1964) 1460.
[13] J. Koike et al., Mater. Sci. Eng. A 213 (1996) 98-102.
[14] C. Schuh, D.C. Dunand, Scripta Mater. 45 (2001) 1415-21.
[15] http://www.sentesoftware.co.uk/biblio.html, A collection of free downloadable papers on the development and application of JMatPro, Sente Software Ltd., 2007
[16] P. Lasne, private communication, Transvalor, France, 2007